J. Phys. Chem. Solids. Pergamon Press 1966. Vol. 27, pp. 1519–1529. Printed in Great Britain.

PHYSICAL BEHAVIOR OF GERMANIUM UNDER SHOCK WAVE COMPRESSION*

R. A. GRAHAM, O. E. JONES and J. R. HOLLAND

Sandia Laboratory, Albuquerque 87115, New Mexico

(*Received* 24 *January* 1966)

Abstract—Shock wave compression measurements from 20 to 140 kb and resistivity measurements under shock wave compression to 40 kb are reported for Ge in the [111] orientation. The Hugoniot elastic limit is found to be 44 ± 4 kb and a phase transition in the pressure range from 114 to 122 kb at about 160°C is identified. The transition occurs at a volume between $0{\cdot}870\ V_0$ and $0{\cdot}880\ V_0$. A shock wave velocity measurement in the mixed phase region allows the slope of the phase diagram to be determined as $-3{\cdot}1 \times 10^{-2}$ kb °C^{-1}. The pressure and volume data are in good agreement with the static work; these data, when combined with the slope of the phase diagram, clearly identify the transition as the solid–solid transition to the white tin structure. The observed exponential decrease of resistivity with elastic strain allows an energy gap change computation which agrees with theoretical calculations for silicon to 60%. Unusual features of the band structure of one-dimensionally strained [111] Ge are discussed. The new technique developed is generally applicable for shock compression and resistivity measurements on semiconductors.

INTRODUCTION

PREVIOUS shock wave compression experiments[1] on single crystal germanium have revealed a complex wave structure resulting from a high Hugoniot elastic limit of about 40 kb and a suspected phase transition at about 130 kb. Because of the high elastic limit, large, elastic one-dimensional compressions are uniquely achieved in shock wave experiments below the Hugoniot elastic limit. Since large elastic compressions can be achieved, measurements of the resistivity of germanium under shock loading conditions in the elastic range may provide a measure of the energy gap change induced by one-dimensional strain and a verification of theoretical calculations[2,3] if the germanium samples behave intrinsically. In addition, resistance-time measurements of shock waves produced by symmetrical projectile impacts provide the basis for a method to determine the stress–volume relation for semiconductors. New techniques are required for these measurements because of the complex wave structure of germanium and the necessity of a close coupling between measurements of the stress and electronic properties.

The purpose of this paper is twofold. Both shock wave compression results and measurements of the resistivity of germanium in one-dimensional strain will be presented. The shock compression results give a measure of the Hugoniot elastic limit and give thermodynamic data which permit the transition to be identified as polymorphic. The resistivity measurements are found to provide an approximate verification of the theoretical predictions. A new experimental technique is described which permits a measurement of both shock compression and resistivity from a common experimental record and avoids the wave interaction problem inherent in free-surface velocity measurements. Section 1 includes a description of the experimental arrangement and an analysis of the form of the predicted resistance–time behavior. The results and a discussion of the stress–volume measurements are presented in Section 2. Finally, Section 3 shows the results of and a discussion of the resistivity measurements. The authors are aware that the manuscript contains results which are normally of interest to readers in different

* This work was supported by the United States Atomic Energy Commission.

physical fields. Section 3 is recommended for those readers principally interested in the effects of strain on the band structure of semiconductors; while Sections 1 and 2 are recommended to those readers principally interested in shock wave compression measurements and high pressure phase diagrams.

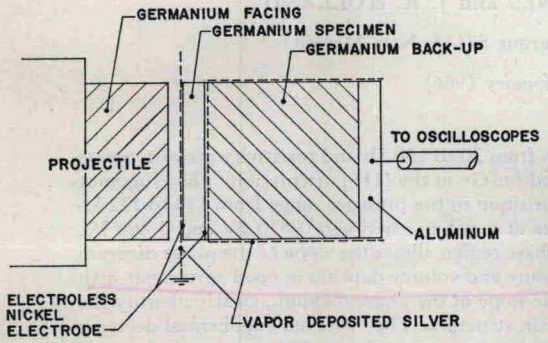

FIG. 1. Schematic drawing of the specimen and impacting projectile.

SECTION 1
EXPERIMENTAL CONSIDERATIONS

Experimental arrangement

Shock loading is accomplished by impacting large diameter-to-thickness ratio disks of germanium upon each other in order to ensure a state of uniaxial strain in all but the periphery of the disks for the duration of the experiment. As shown in Fig. 1, one disk, mounted on the face of a projectile, is accelerated to high velocity by means of a compressed gas gun[4] and is impacted in vacuum upon the specimen disk mounted on the end of the gun. Angular misalignment between the impacting surfaces is about 5×10^{-4} rad.* Germanium backup disks are carefully mated to the rear of the specimen. The thicknesses of the impact and backup disks are chosen so that the stress waves propagate through and out of the specimen disk without reflection until, finally, the specimen is stressed uniformly to the impact value for a brief interval preceding the arrival of unloading waves.

The disks, 38 mm in dia., are cut from single crystals of high purity, *n*-type germanium of nominal 50 Ω-cm resistivity and are oriented with their faces parallel to a (111) crystal plane.[6] Intrinsic behavior at atmospheric pressure was confirmed by the measured *n*-type carrier concentration of 10^{14} cm^{-3}, and resistivity–temperature measurements from 20 to 75°C. The dislocation density was measured to be nominally 6×10^3/cm^2. Depending on the particular experiments, the thicknesses of the specimen disks are 3·2, 4·0 and 8·0 mm.

The resistance–time history resulting from stress waves propagating through the specimen is obtained under constant current conditions. Voltage–time measurements across the thickness of the specimen disk are recorded with a Tektronix 545 oscilloscope. The constant current of 1·00 A is applied to the specimen disk about 500 nsec before impact to prevent resistive heating of the disk. The typical signal level prior to impact is 0·4 V.

Both faces of the disk are entirely electroless nickel plated to provide ohmic electrodes.[7] The impact surface electrode of the specimen is also coated with vapor deposited silver and maintained at ground potential. The backup disk assembly, entirely vapor coated with silver, serves as the circuit lead to the other electrode. As will be shown in the analysis, the resistance change induced by the stress can be read directly from each record. Thus, contact resistance is effectively canceled out unless this contact resistance changes with stress. Since the electrodes are located at known positions, any change of contact resistance with stress would be shown as a change at the specific time that the stress reaches an electrode. No such changes were observed in the stress region below the elastic limit. It is estimated that the resistivity measurement is accurate to ±10%.

Expected resistance–time behavior

For impact stresses in the range of several hundred kb, multiple waves have previously been observed in germanium which indicate the presence of slope discontinuities, or cusps, in the stress–volume relation.[1] To obtain an analytical description of the expected resistance–time behavior, consider a semiconductor disk in which two stress waves of different amplitude and different wave velocity are propagating. As shown in Fig. 2, the disk is divided into zones of different resistivity at any instant of time. The total resistances between the electrodes is then the sum of

* Some of the techniques involved in a gun experiment are discussed in Refs. 4 and 5.

the resistances of the three zones. If we assume (1) that all wave velocities are steady, (2) that all stress amplitudes are steady, (3) that the resistivity is not time dependent, (4) that the stressed regions of the disk are in a state of one-dimensional strain, and

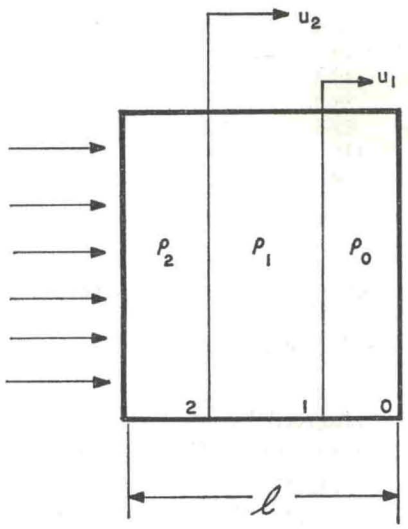

FIG. 2. Three zone resistivity model for a shock-wave loaded semiconductor. Two separate shock waves are shown as would be encountered in the stress region above the Hugoniot elastic limit.

(5) that the strains are infinitesimal;* it follows that:

$$AR(t) = \rho_0 l + U_1 t(\rho_1 - \rho_0) + U_2 t(\rho_2 - \rho_1), \qquad 0 < t < \frac{l}{U_1} \tag{1}$$

and

$$AR(t) = \rho_1 l + U_2 t(\rho_2 - \rho_1), \qquad \frac{l}{U_1} < t < \frac{l}{U_2} \tag{2}$$

where: A is the area of the disk; R is the resistance between the electrodes; ρ is the resistivity; U is the wave velocity; l is the thickness of the disk; t is the time and the subscripts 0, 1 and 2 refer to the various zones.

Equations (1) and (2) show that the electrical resistance between the electrodes of the specimen at any time is equal to the sum of the resistances of the zones. After all the waves have propagated out of the specimen without reflection, the resistance–time record will exhibit a final value corresponding to the impact stress. The initial and final values of the resistance are connected by a continuous line made up of segments of different slope, each segment corresponding to the propagation of a wavefront through the specimen. The initial and final values of the resistance explicitly define the change in resistivity due to the impact stress; the discontinuities in slope show the existence of multiple waves and define transit times for each wave from which the wave velocities can be calculated. This behavior is clearly shown in the typical record given in Fig. 3. Thus, resistance–time measurements can yield explicit data on the number of wavefronts and their wave velocities as well as the resistivity associated with each wave. Further, the complications resulting from wave reflections and subsequent interactions, which are inherent in free surface velocity techniques, are avoided.

Although it was originally hoped that values for resistivity would be obtained for the full stress range and thus provide quantitative data on the resistivities associated with the phase transition and the plastic range, experimental results show an e.m.f. for stress increments above the elastic limit which precludes quantitative resistivity measurements. Also, the temperature rise for large compressions is large and not accurately known such that resistivity is governed by the uncertain temperatures rather than the compression. The resistance–time measurements are sufficient, however, to provide good measurements of the various wave velocities, and quantitative resistivity data is obtained in the elastic range.

In order to determine the stress and specific volume, the particle velocity associated with each wave must be known in addition to the wave velocity. Because of symmetry, the total particle velocity imparted to the specimen disk is one-half the experimentally measured impact velocity.† In general the division of the total particle velocity

* It is not necessary to neglect the particle velocity (strain) to develop the analysis. It has been neglected for illustrative purposes only. All reduced data include the effects of finite particle velocity.

† The instantaneous velocity of the projectile immediately prior to impact is measured to a precision of 0·5%.[8]

Table 1. *Summary of shock wave compression data on* [111] *germanium* $\rho = 5{\cdot}35$ g/cm^3

Shot	u_p[a] (mm/μsec)	No. of waves	U_1 (mm/μsec)	U_2[b] (mm/μsec)	U_3[b] (mm/μsec)	σ_1 (kb)	σ_2[c] (kb)	σ_3[d] (kb)	$(V/V_0)_1$	$(V/V_0)_2$[e]	$(V/V_0)_3$[f]
58	0·0775	1	5·63	—	—	23·3	—	—	0·9864	—	—
59	0·1286	1	5·78	—	—	39·8	—	—	0·9778	—	—
148	0·1580	2	5·63–5·78	3·43	—	c	46·5	—	e	0·9705	—
147	0·1620	2	5·79	3·41	—	c	49·0	—	e	0·9697	—
135	0·1700	2	5·75	3·58	—	c	50·3	—	e	0·9675	—
133	0·2132	2	5·75	3·54	—	c	58·3	—	e	0·9551	—
60	0·3432	2	—	3·63	—	c	83·5	—	e	0·9193	—
149	0·5540	2	5·79	4·13	—	c	136	—	e	0·8748	—
150	0·6015	3	—	4·26	1·17	c	d	142	e	f	0·8413

[a] Particle velocity is taken as $\frac{1}{2}$ the measured impact velocity.
[b] Wave velocity relative to laboratory coordinates.
[c] Stress of the second wave is computed assuming the particle velocity of the first wave is 0·1443 mm/μsec.
[d] Stress of the third wave is computed assuming the particle velocity of the second wave is 0·5778 mm/μsec.
[e] Volume computation assumes particle velocity of first wave is 0·1443 mm/μsec.
[f] Volume computation assumes particle velocity of second wave is 0·5778 mm/μsec.

between multiple waves is unknown for a single experiment; however, if in a series of experiments the total particle velocity is systematically varied in the immediate neighborhood of a suspected cusp in the stress–volume relation until a change in the number of waves is observed, the particle velocity associated with each of the multiple waves is established. The stresses and volumes associated with any multiple wave structure can then be calculated from conservation of mass and momentum relationships,[9] if it is assumed that the particle velocity associated with a cusp is independent of driving pressure.

SECTION 2
SHOCK COMPRESSION RESULTS

Two cusps in the stress–volume relation are revealed in the data summary shown in Table 1. For a particle velocity, u_p, less than 0·1286 mm/μsec a single wave is observed and at $u_p = 0{\cdot}1580$ mm/μsec two waves are observed. Thus, a cusp exists between these two values of particle velocity. From $u_p = 0{\cdot}1580$ mm/μsec to 0·5540 mm/μsec two waves are observed, while at $u_p = 0{\cdot}6015$ mm/μsec three waves are observed.

The first of the two cusps observed and investigated is at a stress of 44 ± 4 kb which corresponds to the transition between elastic and plastic behavior, and the second is at a stress of about 140 kb which we will show is the solid–solid phase transition observed by MINOMURA and DRICKAMER[10] at a pressure of about 120 kb. Before considering the properties of the transition the shock wave compression at lower stresses must be examined.

Hugoniot elastic limit

The leading wave is identified as an elastic wave by comparison of the wave velocity with the low signal wave velocity[12] of 5·54 mm/sec. The wave velocity is somewhat higher than the low signal velocity, but this is to be expected on the basis of the finite compressions in the shock experiment. There is no detectable volume change ($< 0{\cdot}5\%$) associated with the cusp at 44 kb; thus this cusp is clearly not identifiable as a first order phase transition.

The particle velocity of the elastic wave as obtained by other investigators is shown in Table 2. There is a wide variance in values obtained by

Table 2. *Various values for the particle velocity of the elastic wave of* [111] Ge

WACKERLE[11]	MCQUEEN[13]
0·153 mm μsec^{-1}	0·114 mm μsec^{-1}
0·161 mm μsec^{-1}	0·134 mm μsec^{-1}
0·168 mm μsec^{-1}	
0·178 mm μsec^{-1}	

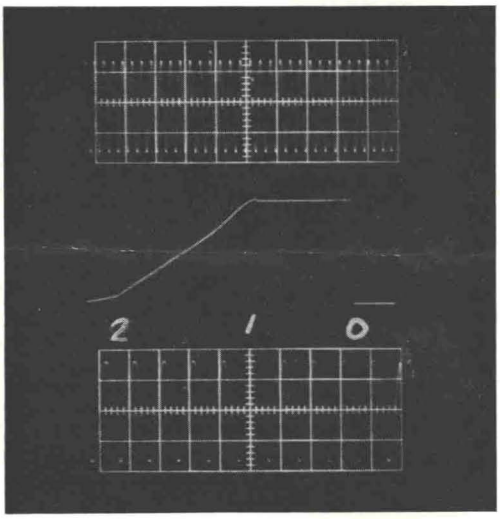

FIG. 3. Typical resistance–time record. Time increases from right to left. The switch closure applying current to the sample occurs at the time marked 0. Impact occurs at the time marked 1. First wave transit time through the sample is marked 2. Second wave transit time is not recorded on this record but is recorded on another oscilloscope with a longer recording time. The upper timing wave is 10 MHz.

[*facing page* 1522

the various investigators and within data obtained by the same investigator. The pronounced stress relaxation observed behind the elastic wave by all the previous investigators suggests that the yield process is quite complex and, as is evident from the data, sensitive to experimental conditions. With our technique of obtaining the Hugoniot elastic limit all measurements are made in direct compression without unloading from free surfaces, and the region around the Hugoniot elastic limit may be investigated for small increments of stress over the critical value rather than for the large input stresses characteristic of an explosive experiment.

Intermediate pressure region

Our data in the stress region intermediate between the two cusps show the usual linear relation between U_s and u_p. In comparing our data to that of other investigators, it should be observed that interpretation of the data from a free surface velocity experiment for a material with a multiple wave structure and time dependent mechanical properties is sensitive to assumptions concerning the various wave interactions and relaxations. Our experiment characterizes the material for the total particle velocity imparted to the material and gives the wave velocity of all waves without complications resulting from the interaction of the waves. Thus the data relating the total particle velocity to wave velocities is obtained with minimum qualification. However, as was previously stated, to compute the stress in the multiple wave region, it must be assumed that the particle velocity of the leading wave is independent of the total particle velocity. This assumption is open to criticism since WACKERLE[14] has observed that the particle velocity and wave velocity of the Hugoniot elastic wave in crystalline quartz increase with increasing driving pressure. However, our wave velocity measurements provide some indication of the amplitude of the leading wave since a change in wave velocity is expected to result from a change in particle velocity. As can be seen in Table 1 the wave velocity of the leading wave was found to be constant with driving pressure. Thus large changes in the amplitude of the elastic wave are not likely. The stress–volume values which result when a constant amplitude elastic wave is assumed are shown in Table 1. Our previous brief report on Ge compares our stress–volume data to that obtained from a free surface velocity technique.[15]

Characteristics of the transition

The large shear component of the elastic wave in the shock experiment results in a transition characterized by a stress rather than by the pressure of the transition. Therefore, we must consider the effect of the elastic compression on the transition. MINOMURA and DRICKAMER[10] have reported that the static transition is insensitive to shear; thus, if this observation is quantitatively correct, we would expect the transition to occur at the same volume regardless of the stress tensor producing the volume change. Our data show that the specific volume at the transition is between $0{\cdot}870\ V_0$ and $0{\cdot}880\ V_0$ when the very small correction to room temperature is made. Thus the transition does occur at the same volume in the static and shock wave experiment since Jamieson's static value[16] for the volume at the transition is $0{\cdot}875\ V_0$.

In order to compute an equivalent pressure from the observed transition stress, several assumptions must be made. Assuming that all stress increments in excess of the Hugoniot elastic limit are hydrostatic (the elastic–plastic assumption) and that the transition pressure is not changed by the shear component, an equivalent hydrostatic pressure may be computed from the observed transition stress. Since it is the volume which is independent of the stress configuration, the equivalent pressure for the elastic range is computed from the volume at the elastic limit and the compressibility. This yields a value from 114 to 122 kb* for the equivalent pressure compared to MIMOMURA and DRICKAMER's[10] value of from 120 to 125 kb. Thus, good agreement is achieved between the static and shock wave compression values for the pressure of the transition.

There has been some question,[1,13] whether the shock induced transition is an anomalous melting and perhaps not the solid–solid transition identified by JAMIESON[16] as a transition to a metallic

* Cusps in the stress–volume curve are located between particle velocity points below and above the cusp. The values shown indicate the range of values possible within the observed points. Consideration of the $U_s - u_p$ values indicates that the cusp is most likely toward the upper end of the range quoted.

white tin structure. Since the shock compression transition is at an elevated temperature ($\sim 160°C$)[13] the small difference in values between the shock transition pressure and quasi-hydrostatic transition pressure indicates that the slope of the pressure–temperature phase diagram is close to zero. This is in agreement with the phase diagram determination for the solid–solid transition reported by BUNDY[17] and indicates that the shock wave transition is polymorphic. This observation is also confirmed by the independent measurement described below.

Slope of the phase diagram

DUFF and MINSHALL[18] have shown that shock wave velocity measurements in the mixed phase region of a shock wave induced polymorphic transition are sufficient to compute the slope of the phase diagram at the particular pressure and temperature of the transition and that this computation is essentially independent of the measurement of the transition pressure. Qualitatively, this unique condition results from the pressure increase which must accompany the volume change associated with the transition if the enthalpy change at the transition is finite.

Our data indicate that the highest stress experiment is in the mixed phase region, since the volume change from the transition stress to the input stress above the transition is not more than 8% while the volume change to complete the transition is 20·7%.[16] Thus the third wave is in the mixed phase region and the slope of the phase diagram may be computed from our measurement of the velocity of this wave. Following Duff and Minshall's development:

$$\left(\frac{dP}{dT}\right)^2 + \frac{2\beta}{(K_c - K)}\frac{dP}{dT} - \frac{C_p}{TV(K_c - K)} = 0, \quad (3)$$

where dP/dT is the slope of the phase diagram, β is the volume coefficient of thermal expansion of the solid before transition, C_p is the specific heat of the solid before transition, T is the temperature, V is the specific volume, K_c is the compressibility of the mixed phase region indicated by the wave velocity measurement and K is the compressibility of the solid before the transition. Using atmospheric pressure values for the thermodynamic parameters and McQueen's temperature rise calculation[13] we find $dP/dT = -3{\cdot}1 \times 10^{-2}$ kb °C^{-1}. The uncertainty involved in using atmospheric pressure values and in the temperature calculation leads to an estimated accuracy of the dP/dT value of 10%. This value of dP/dT is consistent with the comparison of our transition pressure amplitude to the static data. Further, the slope of the phase line is at least an order of magnitude less than the slope of the phase line for the transition from solid to liquid observed statically[17,19,20] and clearly not the solid to liquid transition. The slope of the solid–solid transition phase line is too low for accurate measurements under static conditions; however the measurements indicate that it is negative and very small[17] in agreement with our determination. The present value of dP/dT for the polymorphic transition in Ge appears to be the best measurement made to the present time.

Since values are now available for dP/dT and for the volume change,[16] ΔV, accompanying the transition we can compute the enthalpy change, ΔH, accompanying the transition from the Clausius–Clapeyron relation:

$$\Delta H/\Delta V = T\frac{dP}{dT} \ldots . \quad (4)$$

This change is found to be 12·5 cal/g which when compared to the estimated latent heat of fusion of ~ 110 cal/g for Ge[17] is much too small to be consistent with a melting hypothesis.

In summary, the properties of the shock compression observations when compared to static experiments as in Table 3 clearly illustrate that the shock transition is a solid–solid transition with critical values in agreement with those obtained statically for the transition to the white tin structure. Further, we are able to compute the slope of the phase diagram from wave velocity measurements in the mixed phase region. We find no evidence for intermediate phases[21,22] below the 120 kb transition. Since our experiment includes a large shear strain component the agreement between our values and the static values indicates that the transition is not influenced by shear.

SECTION 3
RESISTIVITY RESULTS

The elastic limit of 44 kb observed in the shock compression experiments results in large (2·5%)

Table 3. Characteristics of the polymorphic transition in Ge

	Static data	Present work
Transition pressure (kb)	120–125[a]	114–122
Specific volume	0·875 V_0[b]	0·870 V_0–0·880 V_0[e]
Temperature (°C)	20	160[c]
$\Delta V/V$	20·7%[b]	—
dP/dT (kb °C^{-1})	—	$-3{\cdot}1\times10^{-2}$
ΔH (cal g^{-1})	—	12·5[d]

[a] Ref. 10.
[b] Ref. 16.
[c] As estimated by McQueen, Ref. 13.
[d] Calculated using ΔV given by Jamieson, Ref. 16.
[e] Corrected to 20°C for comparison with static data.

one-dimensional elastic compressions which are uniquely achieved in the shock wave loading experiments. Resistivity measurements for large uniaxial elastic strains are of interest since they may be useful for confirming the theoretical calculations of KLEINMAN[2] and GOROFF and KLEINMAN[3] which predict the effect of a general strain tensor on the energy bands of silicon, and by inference, germanium. These measurements may also help to describe the so-called "anisotropic stress effect" observed for stressed semiconductor *p–n* junctions.[23]

The component of the energy gap change induced by volumetric compression has been verified by hydrostatic experiments, but the component of energy gap change induced by shear strain has not been verified since large shear strain components cannot be applied statically to brittle materials such as germanium. If the germanium samples behave intrinsically for large shear strain, it is possible that the resistivity measurements under shock compression can provide a measure of the energy gap change induced by shear strain. The conditions imposed on the sample by plane-wave shock loading in the elastic range are well defined allowing all stress and strain components to be accurately evaluated. Further, since the compressions are small the process is adiabatic to a very close approximation and accurate calculations can be made of the slight temperature rise (5·6°K at 44 kb)* induced by shock wave.

* The temperature of the shocked Ge in the elastic range is computed as $T = T_0(V_0/V)^{\gamma}$. Gruneisen's ratio, γ, was taken as 0·725 in agreement with the data of Ref. 24.

Previous attempts to measure energy gap changes induced by shear strain have included the measurement of reflectance from Ge samples subjected to bending stress.[25] Also, piezo-resistance measurements in uniaxial *stress* on heavily doped germanium specimens give deformation potential determinations on the motion of individual valley minima and the valence band maximum.[26] WORTMAN *et al.*[27] have used GOROFF and KLEINMAN's[3] theoretical predictions for silicon to predict the effect of various stress tensors on the band structure of germanium and thus the effect upon the characteristics of Ge *p–n* junctions. IMAI and UCHIDA[28] find this analysis to be consistent with their measurements of the characteristics of heavily doped Ge *p–n* junctions under uniaxial *stress*. Similarly, RINDNER[23] has applied uniaxial *stress* to Ge *p–n* junctions and found agreement in sign and qualitative behavior to that predicted by Wortman *et al.*

The effect of *pressure* on the resistivity of Ge has been extensively investigated and recently summarized in the excellent review by PAUL and WARSCHAUER.[29] The energy gap, E_g, is found to increase linearly with *pressure* to 15 kb at a rate of 5×10^{-3} eV kb^{-1}. From 15 kb to 30 kb the rate of increase of E_g decreases significantly. This has been shown to be consistent with the hypothesis that the minimum energy of the conduction band is shifted in k space. Further, effective mass changes of electrons with *pressure* are found to be only $\frac{1}{2}$% per kb, and the mobility of electrons is found to decrease only 0·4% per kb in the absence of intervalley scattering. Considerable correlation is found between the *pressure* dependence of any

particular gap among all the diamond semiconductors; hence, the analysis of Goroff and Kleinman might be expected to predict the behavior of Ge under *pressure*. This is not to imply that the behavior under shear strain is analogous between Ge and Si, since there is insufficient theoretical or experimental evidence to make this judgment.

The energy band structure for germanium is shown schematically in Fig. 4. The analysis of Goroff and Kleinman for silicon predicts that the

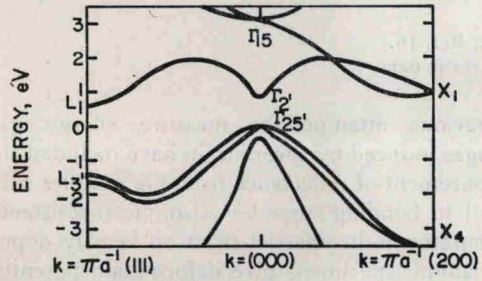

FIG. 4. Band structure of germanium. After Paul and Warschauer, Ref. 28.

conduction band minimum $L_1(111)$ is lowered with [111] one-dimensional strain,* that the degenerate $\Gamma'_{25(j=3/2)}$ valence band maximum is raised with [111] strain and that these positions retain their critical position in the band structure. The predictions are that the change, δ, in energy levels is:

$$\delta L_1(111) = 6{\cdot}20\Delta - 11{\cdot}5\epsilon, \tag{5}$$

and

$$\delta\Gamma'_{25(j=3/2)} = 2{\cdot}09\Delta + 2{\cdot}79\epsilon, \tag{6}$$

* A one-dimensional strain along the [111] axis as achieved in the shock wave experiment gives a strain tensor referred to the crystal axes of:

$$\frac{\epsilon}{3}\begin{bmatrix}1&1&1\\1&1&1\\1&1&1\end{bmatrix} = \frac{\epsilon}{3}\begin{bmatrix}1&0&0\\0&1&0\\0&0&1\end{bmatrix} + \frac{\epsilon}{3}\begin{bmatrix}0&1&1\\1&0&1\\1&1&0\end{bmatrix}$$

$$= \Delta + \frac{\epsilon}{3}\begin{bmatrix}0&1&1\\1&0&1\\1&1&0\end{bmatrix}$$

where ϵ is the strain along the [111] axis. This strain tensor is a combination of a dilatation, Δ, and a dilatationless shear strain.

where Δ is the dilatation and ϵ is the [111] direction strain. The first terms show the effect of the dilatation, and the second terms are due to the dilatationless shear strain. Thus the change in energy gap, δE_g, is predicted to be:

$$\delta E_g = +4{\cdot}11\Delta - 14{\cdot}29\epsilon. \tag{7}$$

The shear strain contribution is clearly dominant for [111] one-dimensional strain. The dilatation part of the expression has been previously measured by PAUL and BROOKS,[30] hence, we look to our measurements for an evaluation of the shear strain contribution.

The results of the resistivity measurements in the elastic range are shown in Fig. 5 where the logarithm of the observed resistivity at wave transit time is plotted against strain. The logarithm of resistivity shows a linear decrease with strain indicating that the decrease of resistivity is due to an exponential term.

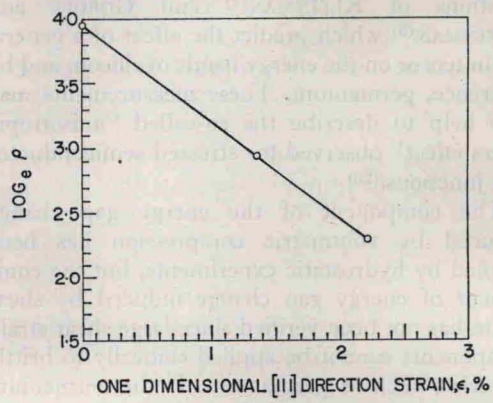

FIG. 5. Resistivity of [111] Ge in one-dimensional strain.

Since the intrinsic resistivity of a semiconductor is related to the energy gap by an exponential term, $\exp[E_g/2kT]$ and the terms involving the mobilities and effective masses of the carriers are pre-exponential factors, the exponential decrease of resistivity with strain indicates that the change is principally due to the strain-induced energy gap change. Assuming that the strained Ge exhibits intrinsic behavior and that the pre-exponential factors affecting the resistivity are unchanged from their atmospheric pressure values, an energy gap change can be calculated consistent with the measured resistivity. The value obtained is

$-4{\cdot}0$ eV/unit strain. Since the energy gap change due to the dilatational component has been evaluated to be $+3{\cdot}7$ eV/unit strain,* the shear strain contribution is $-7{\cdot}7$ eV/unit strain. This is a factor of $1{\cdot}85$ smaller than the theoretical value of $-14{\cdot}29$ eV. Thus, this measurement on Ge agrees with the sign and order of magnitude of the theoretically predicted change for Si.

Although the agreement given above is satisfactory considering the complexity of the problem, somewhat better agreement is achieved by a more detailed examination of the data. The experiment at a strain of $1{\cdot}36\%$ is well below the elastic limit and therefore in a stress region where mechanical relaxation effects are unlikely. The resistance–time record, however, exhibits an increasingly greater downward slope rather than the constant slope expected from the analysis. The curvature is more pronounced early in time and thus is not that expected from the stress unloading behavior from the lateral edge of the sample. Thus, the most likely interpretation of the nonlinear behavior is that equilibrium of carriers is not fully established and that relaxation times are of the order of 10^{-7} sec. The observed resistive behavior tends toward a constant slope late in time; hence, to establish a value for the equilibrium resistivity, the slope of the resistance–time record for late times is extrapolated for full wave transit time.† This yields a resistivity which gives a value of δE_g of $5{\cdot}3$ eV per unit strain. This value of δE_g gives a shear strain contribution for [111] one-dimensional strain of $9{\cdot}0$ eV per unit strain which is a factor of $1{\cdot}6$ smaller than the theoretical value for silicon. Thus, it appears that our best value for the [111] shear strain contribution is 60% lower than that predicted for Si. Considering the uncertain nature of the assumptions concerning the transport properties of the strained Ge and the unknown applicability of the theoretical analysis to Ge, the agreement is considered to be satisfactory. However, further interpretations seem in order.

Results of the extensive work which has been accomplished with hydrostatically strained Ge furnish a comparative background which hopefully might have relevance to the analysis of the current work. However, several major differences exist between the band structure of hydrostatically strained Ge and Ge under [111] one-dimensional strain. As indicated in Fig. 6, the conduction band structure for [111] one-dimensional strain is much simplified. The $L_1(111)$ level is lowered considerably, while the $L_1(1\bar{1}\bar{1})$, $L_1(\bar{1}1\bar{1})$ and $L_1(11\bar{1})$ levels are raised at a rapid rate. Hence, the effect is to change the multivalley semiconductor to a simpler single-valley semiconductor in which all of the electrons are confined to the [111] valley. Further, the nonlinear band gap change indicated for *pressure* greater than 15 kb would not be expected to occur, since detailed analysis[31] of the interband scattering of electrons showed that the effect was caused by the conduction band minima in the [100] direction moving closer in energy to the [111] minima thus causing significant interband scattering. In the one-dimensional strain configuration these two minima are further apart in energy in the strained state than in the unstrained state; thus no intervalley scattering would be expected.

On the other hand, the valence band structure becomes more complex in the one-dimensional strain state than in the hydrostatic state. One-dimensional [111] strain causes the $\Gamma'_{25(j=3/2)}$ edge to be split at a rapid rate. Further, the $\Gamma'_{25(j=1/2)}$ band, originally at the same energy as the $j = 3/2$ level, changes energy with a different coefficient than either of the split $j = 3/2$ levels. Thus, three distinct valence band energy levels exist at the same momentum value for which one level exists in the unstrained and the hydrostatic state.

The band gap for Ge in [111] one-dimensional strain is predicted to be narrowed from $0{\cdot}66$ eV to $0{\cdot}46$ eV at 2% strain. Because of this, deeper lying impurity levels unimportant in the unstrained or hydrostatic state are possibly more important in the uniaxial strain state. Hence, it is clear that because of these several major differences in band structure, results and conclusions concerning conductivity of hydrostatically strained Ge are of marginal applicability to the analysis of [111] one-dimensionally strained Ge.

Noting the simplicity of the one-dimensionally strained conduction band, it is interesting to use the position of the L_1 minimum as a reference and compute the effective energy level of the valence

* A bulk modulus of $7{\cdot}49 \times 10^2$ kb was used to calculate the volume dependence from the measured pressure dependence[30] of the energy gap.

† Wave transit time for this sample is $1{\cdot}42$ μsec.

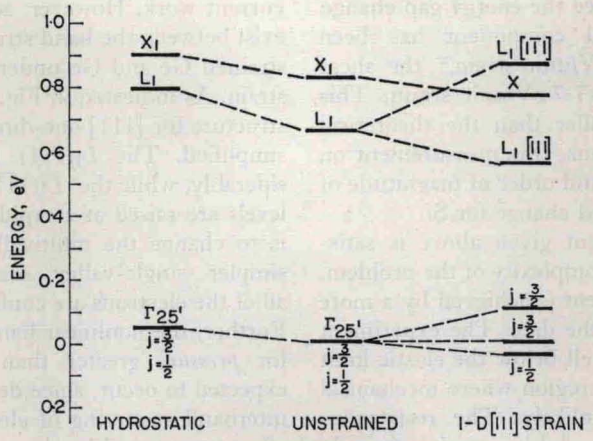

FIG. 6. Diagram of the effect of a 2% hydrostatic compression and a 2% one-dimensional [111] compression on critical points in the band structure. Values shown are calculated from the analysis of GOROFF and KLEINMAN.[3]

band maximum from the calculated energy gap change obtained from our experimental results. This computation suggests that the effective valence band maximum is essentially stationary in energy as if splitting of the valence band edge results in a new distribution of holes among the closely spaced valence band energy levels whose behavior approximates the original unstrained behavior. However, the physical significance of this observation is not clear, since data describing the populations of the various valence band energy levels, hole mobilities and effective masses for Ge in [111] one-dimensional strain are necessary to provide data for a more complete analysis. The large change in the effective mass of holes for Si under uniaxial *stress*[32] suggests that significant changes are to be expected.

The source of the finite time to establish equilibrium resistivity is not apparent from previously measured relaxation times of carriers. Intervalley relaxation times have been measured by high frequency ultrasonic absorption of shear waves[33] and are about 10^{-11} sec at room temperature and for low carrier densities. Similarly, the relaxation time for the repopulation of holes is of the same order of magnitude or shorter. Thus, the observed resistivity relaxation is most likely due to impurity scattering or generation–recombination times.

In summary, the resistivity measurements in elastic one-dimensional strain provide a measure of an effective coefficient of energy gap change with [111] one-dimensional strain if atmospheric pressure values for mobilities and effective masses are assumed for the strained crystal. The coefficient determined gives a shear strain contribution which agrees to 60% with the theoretically predicted value for Si. However, further experiments in one-dimensional strain are required for a more complete physical description of the conduction process. Our results indicate that shock waves in the elastic region provide a convenient deformation for the study of the change in the band gap of Ge by shear strain.

Acknowledgment—The authors are pleased to acknowledge exploratory experiments by W. J. HALPIN and W. B. BENEDICK, the excellent technical assistance of G. E. INGRAM, the copy of Ge data from Dr. JERRY WACKERLE, carrier concentration measurements by Dr. J. KENNEDY, and many useful discussions with Dr. G. E. SEAY and other colleagues at Sandia Laboratory.

REFERENCES

1. McQUEEN R. G., MARSH S. P. and WACKERLE J., *Bull. Am. Phys. Soc.* **7,** 447 (1962).
2. KLEINMAN L., *Phys. Rev.* **128,** 2614 (1962).

3. GOROFF I. and KLEINMAN L., *Phys. Rev.* **132,** 1080 (1963).
4. THUNBORG S., INGRAM G. E. and GRAHAM R. A., *Rev. Scient. Instrum.* **35,** 11 (1964).
5. HALPIN W. J., JONES O. E. and GRAHAM R. A., *Symposium on Dynamic Behavior of Materials.* ASTM Special Technical Publication No. 336, (1963).
6. Supplied by Knapic Electro-Physics, Inc.
7. SULLIVAN M. V. and EIGLER J. H., *J. Electrochem. Soc.* **104,** 226 (1957).
8. INGRAM G. E., *Rev. Scient. Instrum.* **36,** 458 (1965).
9. DUVALL G. E., *Response of Materials to High Velocity Deformation*, p. 165. Interscience, New York (1961).
10. MINOMURA S. and DRICKAMER H. G., *J. Phys. Chem. Solids* **23,** 451 (1962).
11. WACKERLE J., private communication, Los Alamos Scientific Laboratory.
12. MASON W. P., *Physical Acoustics and the Properties of Solids.* D. Van Nostrand, New York (1958).
13. MCQUEEN R. G., *Metallurgy at High Pressures and High Temperatures.* Gordon and Breach (1964).
14. WACKERLE J., *J. Appl. Phys.* **33,** 922 (1962).
15. GRAHAM R. A., JONES O. E. and HOLLAND J. R., *J. Appl. Phys.* **36** 3955 (1965).
16. JAMIESON J. C., *Science* **139** 762 (1963).
17. BUNDY F. P., *J. Chem. Phys.* **41,** 3809 (1964).
18. DUFF R. E. and MINSHALL F. S., *Phys. Rev.* **108,** 1207 (1957).
19. HALL H. T., *J. Phys. Chem.* **59,** 1144 (1955).
20. BUNDY F. P. and STRONG H. M., *Solid State Physics* **13,** p. 131. Academic Press, New York (1962).
21. BATES C. H., DACHILLE F. and ROY R., *Science* **147,** 860 (1965).
22. BUNDY F. P. and KASPER J. S., *Science* **139,** 340 (1963).
23. RINDNER W., *J. Appl. Phys.* **36,** 2513 (1965).
24. GIBBONS D. F., *Phys. Rev.* **112,** 136 (1958).
25. PHILLIPS H. R., DASH W. C. and EHRENREICH H., *Phys. Rev.* **127,** 762 (1962).
26. FRITZCHE H., *Phys. Rev.* **115,** 336 (1959).
27. WORTMAN J. J., HAUSER J. R. and BURGER R. M., *J. Appl. Phys.* **35,** 2122 (1964).
28. IMAI T. and UCHIDA M., *Japan J. Appl. Phys.* **4,** 409 (1965).
29. PAUL W. and WARSCHAUER D. M., *Solids Under Pressure*, p. 179. McGraw-Hill, New York (1963).
30. PAUL W. and BROOKS H., *Phys. Rev.* **94,** 1128 (1954).
31. NATHAN M. I., PAUL W. and BROOKS H., *Phys. Rev.* **124,** 391 (1961).
32. HENSEL J. C. and FEHER G., *Phys. Rev.* **129,** 1041 (1963).
33. MASON W. P. and BATEMAN T. B., *Phys. Rev.* **134,** A1387 (1964).